

Study of Local Fields of Dendrite Nanostructures in Hot Spots Formed on SERS-Active Substrates Produced via Template-Assisted Synthesis

E. P. Kozhina^{a, *}, S. N. Andreev^{a, b}, V. P. Tarakanov^c, S. A. Bedin^{a, d},
I. M. Doludenko^d, and A. V. Naumov^a

^aMoscow Pedagogical State University, Moscow, 119435 Russia

^bMoscow Polytechnic University, Moscow, 107023 Russia

^cJoint Institute for High Temperatures, Russian Academy of Sciences, Moscow, 125412 Russia

^dFederal Research Center “Crystallography and Photonics,” Russian Academy of Sciences, Moscow, 119333 Russia

*e-mail: Liza.kozhina.99@mail.ru

Received July 15, 2020; revised August 10, 2020; accepted August 26, 2020

Abstract—A procedure is proposed for template-assisted synthesis on track membranes using iodide electrolyte to produce substrates with dendritic nanostructures formed on the tips of silver nanowires. The distribution of the electromagnetic field near a silver nanorhombus irradiated with visible laser radiation is modeled because the dendrite branches are rhombus-shaped nanoparticles. Calculations indicate considerable enhancement of the local electric fields near the sharp tops of the nanorhombus.

DOI: 10.3103/S1062873820120205

INTRODUCTION

Nanostructures made of precious metals are of special interest in giant Raman scattering (SERS, or surface-enhanced Raman scattering), due to their resonant behavior in the optical range [1]. The extremely high electromagnetic field amplification associated with plasmon resonance plays an important role in the amplification of the Raman signal of molecules adsorbed in domains with high scattering capacity (also known as hot spots) [2, 3]. There are currently a number of synthesis procedures and ways of manufacturing metallic nanoparticles with different shapes. The modeling of local electric fields near the surfaces of such structures allows us to study the nature of SERS signal amplification in the domain of hot spots. When studying the influence of local fields, it is important to consider their fluctuations in dielectric solutions [4, 5] and the results from concentration effects [6, 7]. The parameters of amplification can therefore vary from molecule to molecule.

Hot spots can arise between adjacent plasmon nanostructures if they are less than 4 nm from one another and form near single nanosized particles with high surface curvature (e.g., on the poles of a nanosphere, or on the tips of nanorods and nanotriangles because of the glowing peak effect) [3, 8, 9]. A substantial increase in the intensity of the electric field is then observed, due to the electric component of an electromagnetic field being concentrated on nano-

sized peaks or irregularities. Examples of such structures include substrates with arrays of nanowires (NWs) on their surfaces [10, 11].

Since the optical properties of metallic nanostructures depend not only on their size but largely on the shape as well, nanoparticles with irregular shapes (e.g., polyhedrons) display more unique physical properties than nanostructures of simple shape (spheres or rods) [12]. Triangle-shaped nanoparticles thus exhibit not only the effect of multiple plasmon resonances, but the strong amplification of local fields on sharp tips of a triangle as well (in contrast to an ellipsoid) [13]. Strong amplification can also be achieved in a gap of less than 3 nm between two nanotriangles. This is explained by the more complicated spectrum of resonance for interacting structures, in which the number and magnitude of different resonances depend on the direction of irradiation and the distance between particles [14, 15].

Strong amplification of SERS signals can also be obtained on a more developed surface of a substrate, since the area of the contact surface does not increase (e.g., on substrates with highly-branched dendritic nanostructures that amplify electric fields in a wide spectral range). It has been shown that more branched surfaces provide the strongest amplification of SERS signals, and electric fields reach their maximum values at the vertices of dendrite branches (sharp tips), and at points where multilayer dendritic branches are in con-

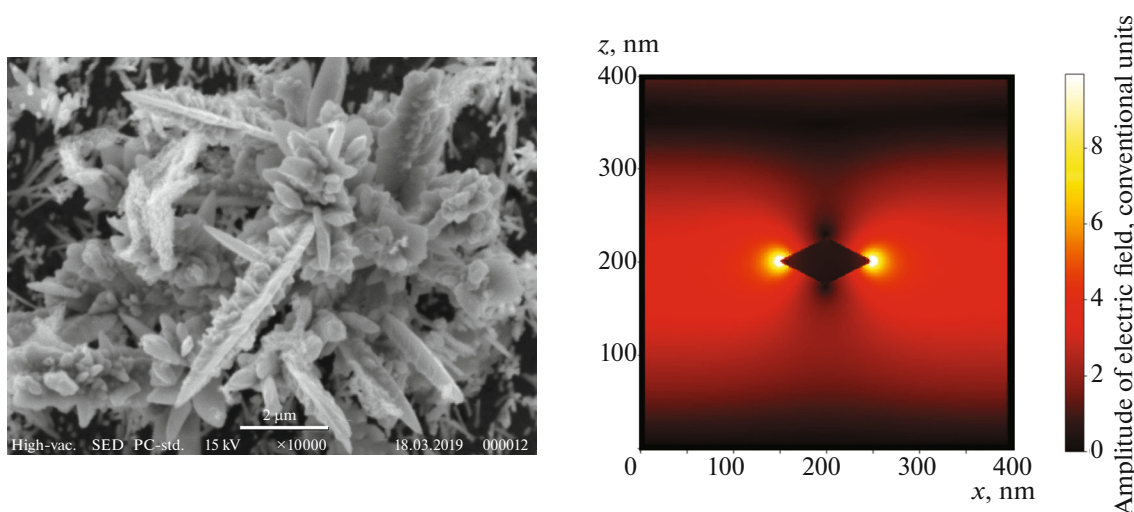


Fig. 1. (a) Image of a dendrite nanostructure with branches, obtained on a raster electronic microscope. (b) Distribution of the coefficient of amplification (E/E_0) of an electric field near a nanorhombus.

tact with one another [16, 17]. Compared to simple irregular silver substrates, dendritic nanostructures made of silver have a great many hot spots, ensuring strong amplification of SERS signals. Such structures can be produced via galvanic displacement [18], along with the simpler and cheaper technique of electrochemical deposition in power of a porous aluminum oxide [19–21].

In this work, we propose manufacturing substrates with dendritic nanostructures formed on the vertices of silver NWs via template synthesis with iodide-containing electrolyte on tracking membranes (TMs). The advantage of using TM is that we can vary the diameter of pores and, in contrast to porous aluminum oxide, TMs do not have a high density of pores; as a result, dendritic nanostructures do not form layers on one another, preserving the unique pattern of hot spots on a surface. This allows optimization of the density of pores in order to form more hot spots. Since branches of dendrites are rhombus-shaped nanoparticles, we modeled the distribution of an electromagnetic field near a silver nanorhombus irradiated with a laser in the visible range. Calculations indicate local amplification of electric fields near the vertices of the nanorhombus.

EXPERIMENTAL

Substrates with dendritic nanostructures formed on the vertices of silver NWs were prepared via pattern synthesis. A polymer TM 12 μm thick with a pore diameter of 100 nm and a surface pore density of 10^8 cm^{-2} was used as a synthesis template. Pores in the TM were filled with silver [22].

Iodide-containing silvering electrolyte (metallic silver, 15–20 g/L; potassium iodide, 230–300 g/L [23, 24]) was used in this work. Deposition was done

at room temperature with a constant current density of 80 to 250 mA/cm^2 through the pores of the TM. By varying the period of deposition from 10 to 100 s, we achieved complete filling of pores in the polymer template with metal emerging on its surface in the form of dendritic structures (Fig. 1a). When electrochemical deposition was complete, the polymer matrix was removed by dissolving it in a concentrated alkali solution (25% NaOH).

The amplification of local electromagnetic fields near nanorhombus was modeled mathematically using the fully electromagnetic KARAT code [25] in planar geometry (X, Z). The domain of calculation was a square 400 by 400 nm in size. In the center of the square, there was a silver nanoparticle in the form of a rhombus with large diagonal of 100 nm along X axis, and a small diagonal of variable length (10 to 100 nm) along the Z axis.

We used a Drude model with parameters for silver [26] to describe the electromagnetic properties of a nanoparticle: plasma frequency, 8.78 eV; constant of attenuation, 0.02 eV. Laser irradiation with flat polarization (E_x, B_y) and a wavelength of 785 nm propagated in the positive direction of the Z axis and interacted with the nanorhombus, resulting in a local change in the electromagnetic field of incident radiation in the domains near its vertices. As an example, Fig. 1b shows the distribution of the coefficient of electric field amplification (E/E_0) near a nanorhombus of 100 by 50 nm, where E_0 is the amplitude of the electric field of incident radiation. It can be seen in Fig. 1b that there was considerable amplification on the acute vertices of the rhombus, while it attenuated on obtuse vertices. Figure 2a shows the dependence of the coefficient of electric field amplification (E/E_0) at points on the continuation of the rhombus's diagonals

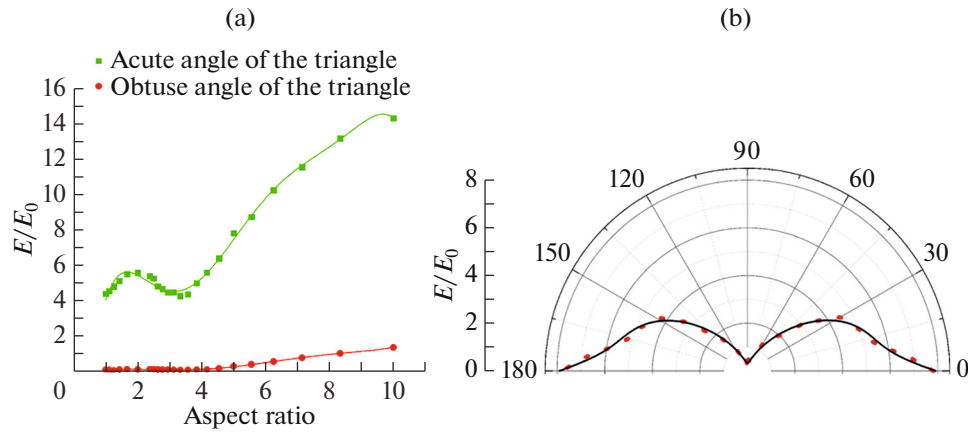


Fig. 2. (a) Dependence of the coefficient of the amplification of an electric field on the aspect ratio of the diagonals of a nanorhombus in spots near a vertex with an acute angle and one with an obtuse angle. (b) Dependence E/E_0 on the angle of rotation of the large diagonal of a nanorhombus with respect to the vector of the electric field of the incident radiation.

at a distance of 2 nm from its vertices on the aspect ratio of its diagonals (d).

When $d > 3$, we observe a general tendency of both vertices: the higher the aspect ratio, the stronger the field amplification. There is a local maximum (E/E_0) when $1 < d < 3$, but it is much lower when $d > 4$ than the coefficient of amplification when $d > 4$. Near the vertex of the rhombus with an acute angle, E/E_0 thus reaches a value of 14 when $d = 10$. As noted above, there is virtually no amplification of the field near the vertex of the rhombus with an obtuse angle, and E/E_0 is greater than 1 only when $d > 8$.

Both the aspect ratio of the rhombus's diagonals and its dislocation with respect to incident radiation are important parameters for the local amplification of the electric field. Silver nanoparticles were modeled in the form of a rhombus with large diagonal of 100 nm and small diagonal of 20 nm. The coefficient of amplification was determined for a point at a distance of 2 nm from a vertex with an acute angle on the continuation of the rhombus's large diagonal. Figure 2b shows the dependence of E/E_0 on the angle of rotation of the rhombus's large diagonal with respect to the vector of the electric field of the incident radiation. It can be seen that the field amplification is maximal if the large diagonal is parallel to the vector of electric field E , but the coefficient of amplification tends toward zero if the large diagonal is perpendicular to field vector E .

We obtained metallic substrates made of silver with dendrites on their surfaces in the form of nanorhombi. Interaction between a nanorhombus and laser radiation of the visible spectrum in planar geometry was modeled, and the local distribution of electric fields near the vertices of the nanorhombus was studied using the KARAT fully electromagnetic 3D code. We found there was strong amplification of electric field on acute vertices, while it was attenuated on obtuse

ones. We obtained the dependence of the coefficient of electric field amplification on aspect ratio d of the diagonals of a rhombus, and showed in particular that when $d > 3$, the coefficient of field amplification grows along with the aspect ratio. The coefficient of field amplification also depends on the orientation of the nanorhombus with respect to the direction of the intensity of the electric field of the incident radiation: if the large diagonal of the rhombus is parallel to the vector of the electric field's intensity, the amplification of local electric field will be maximal. The maximum efficiency of the local amplification of the field will thus be displayed by the rhombus-shaped edges of dendrites with acute angles oriented in parallel to the electric component of the incident laser radiation.

ACKNOWLEDGMENTS

The measurements were made using equipment at the shared resource center of the Russian Academy of Sciences' Center "Crystallography and Photonics."

FUNDING

This work was performed as part of a State Task for Moscow State Pedagogical University on the topic "Physics of Nanostructured Materials: Fundamental Research and Applications in Materials Science, Nanotechnology, and Photonics."

REFERENCES

1. Radziuk, D. and Moehwalda, H., *Phys. Chem. Chem. Phys.*, 2010, vol. 17, p. 21072.
2. Etchegoina, P.G. and Le Ru, E.C., *Phys. Chem. Chem. Phys.*, 2008, vol. 10, p. 6079.
3. Kuttner, C., Plasmonics in sensing: From colorimetry to SERS analytics, in *Plasmonics*, Gric, T., Ed., IntechOpen, 2018.

4. Naumov, A.V., Gorshchev, A.A., Gladush, M.G., et al., *Nano Lett.*, 2018, vol. 18, p. 6129.
5. Gladush, M.G., Anikushina, T.A., Gorshchev, A.A., et al., *J. Exp. Theor. Phys.*, 2019, vol. 128, no. 5, p. 655.
6. Eskova, A.E., Arzhanov, A.I., Magaryan, K.A., et al., *Bull. Russ. Acad. Sci.: Phys.*, 2020, vol. 84, no. 1, p. 40.
7. Eskova, A.E., Arzhanov, A.I., Magaryan, K.A., et al., *EPJ Web Conf.*, 2019, vol. 220, 03014.
8. Ostroukhov, N., Sleptsov, V., Tyanginskii, A., et al., *Fotonika*, 2011, no. 5, p. 38.
9. Karpov, S., *Fotonika*, 2012, no. 3, p. 52.
10. Kozhina, E.P., Bedin, S.A., Razumovskaya, I.V., et al., *J. Phys.: Conf. Ser.*, 2019, vol. 1283, 012009.
11. Ermushev, A.V., Mchedlishvili, B.V., Oleinikov, V.A., et al., *Quantum Electron.*, 1993, vol. 23, p. 435.
12. Hu, J., Wang, Z., and Li, J., *Sensors*, 2007, no. 7, p. 3299.
13. Kottmann, J.P., Martin, O.J.F., Smith, D.R., et al., *Opt. Express*, 2000, vol. 6, no. 11, p. 213.
14. Simeone, D., Esposito, M., Scuderi, M., et al., *ACS Photonics*, 2018, vol. 5, no. 8, p. 3399.
15. Merlen, A. and Lagugné-Labarthe, F., *Appl. Spectrosc.*, 2014, vol. 68, no. 12, p. 1307.
16. Orságová Králová, Z., Oriňak, A., Oriňaková, R., et al., *J. Biomed. Opt.*, 2018, vol. 23, no. 7, 075002.
17. Ye, Y., Chen, C., Hua, H., et al., *Cell Rep. Phys. Sci.*, 2020, vol. 1, no. 3, 100031.
18. Yakimchuk, D.V., Kaniukov, E.Yu., Lepeshov, S., et al., *J. Appl. Phys.*, 2019, vol. 126, no. 23, 233105.
19. Rafailović, L.D., Gammer, C., Srajer, J., et al., *RCS Adv.*, 2016, vol. 6, no. 40, p. 33348.
20. Gutés, A., Carraro, C., and Maboudian, R., *J. Am. Chem. Soc.*, 2010, vol. 132, no. 5, p. 1476.
21. Cheng, Z.-Q., Li, Z.-W., Xu, J.-H., et al., *Nanoscale Res. Lett.*, 2019, vol. 14, 89.
22. Bedin, S.A., Rybalko, O.G., Polyakov, N.B., et al., *Inorg. Mater.: Appl. Res.*, 2010, vol. 1, p. 359.
23. Burkat, G.K., *Elektroosazhdenie dragotsennykh metallov* (Electrodeposition of Precious Metals), St. Petersburg: Politekhnik, 2009.
24. Fourcade, F. and Tzedakis, T., *J. Electroanal. Chem. Interfacial Electrochem.*, 2000, vol. 493, p. 20.
25. Tarakanov, V.P., *EPJ Web Conf.*, 2017, vol. 149, 04024.
26. Johnson, P.B. and Christy, R.W., *Phys. Rev. B: Solid State*, 1972, vol. 6, p. 4370.

Translated by K. Gumerov